The Canadian Mineralogist
Vol. 42, pp. 1079-1096 (2004)

GOLD EMPLACEMENT AND HYDROTHERMAL ALTERATION IN METABASIC ROCKS AT THE MOUSKA MINE, BOUSQUET DISTRICT, ABITIBI, QUEBEC, CANADA

ABDELHAY BELKABIR§

Département de Géologie, Faculté des Sciences et Techniques de Marrakech, B.P. 549, Avenue Abdelk. Khattabi, 40 000, Marrakech, Maroc

CLAUDE HUBERT AND LARRY D. HOY

Département de Géologie, Université de Montréal, C.P. 6128, Succursale Centre-Ville, Montréal, Québec H3C 3A7, Canada

ABSTRACT

The Mouska mine, in the Bousquet region of the Abitibi greenstone belt, Quebec, exploits a sulfide-rich quartz-vein-type gold deposit hosted by a metavolcanic sequence of basalt and andesite. The ore zones constitute three main structural and lithologic systems, named 07, 08 and 22, comprising both lenses of massive and disseminated sulfides and quartz veins. Gold, varying from microscopic to visible, is hosted by both sulfide and quartz veins. The ore minerals consist of pyrrhotite and chalcopyrite, together with minor amounts of pyrite. Pyrite in particular, consists of two generations. Pyrite I is fine-grained (100 to 200 μm), and encloses micro-inclusions of gold (10 to 12 μm), chalcopyrite and pyrrhotite. Pyrite II is late, coarse-grained and cataclastic, and lacks micro-inclusions of gold. Pyrite I is rare, and partially to completely replaced by chalcopyrite and pyrrhotite. It may well represent a remnant of the first paragenetic assemblage (with chalcopyrite and pyrrhotite inclusions) in the deposit. Gold in the Mouska deposit exhibits a wide range of occurrences and habits. The gold micro-inclusions in pyrite I contain 4 to 6% Ag; gold in any other habit contains up to 25% Ag. Compared to the common Archean auriferous quartz-vein deposits, the Mouska deposit has a higher sulfide content of the veins, and the variably altered and deformed metabasic rocks show both distal and proximal halos of alteration. Such halos result from a complex and progressive interaction between hydrothermal-predeformational (sulfide event) and tectonometamorphic (quartz event) imprints. Mineralogical, geochemical and isotopic studies show that alteration assemblages surrounding the ore zones not only vary with lithology (basalt to andesite), but indicate a complex hydrothermal history, where the mafic protoliths have undergone several transformations during the Au–sulfide and Au–quartz depositions. In the proximal alteration, the mass-balance calculations display a clear addition of K, which may account for the observed enrichment in biotite and white mica toward the ore zones. However, these calculations show substantial addition of SiO_2 only in the altered basalts, which can be explained by the massive destruction of ferromagnesian minerals.

Keywords: gold, quartz veins, sulfide veins, hydrothermal alteration, Mouska mine, Abitibi belt, Quebec.

SOMMAIRE

Le gisement d'or exploité à la mine Mouska, région de Bousquet, ceinture de roches vertes de l'Abitibi, est un dépôt à veine de quartz aurifères riches en sulfures, encaissées dans une séquence métavolcanique de basalte et andésite. Les zones de minerai forment trois systèmes structuraux et lithologiques, nommés 07, 08 et 22, comprenant des sulfures, en lentilles massives et en disséminations, ainsi que des veines de quartz. L'or, variant de microscopique à visible, se retrouve aussi bien dans la minéralisation sulfureuse que quartzique. Le minerai est constitué de pyrrhotite et de chalcopyrite associé à des teneurs faibles de pyrite. La pyrite, en particulier, montre deux générations: la pyrite I, à grains fins (100 à 200 μm), renferme des inclusions d'or (10 à 12 μm), de chalcopyrite et de pyrrhotite. La pyrite II est tardive, à grain grossier (jusqu'à 0.5 mm), typiquement fracturée et pauvre en inclusions. Comparée à la pyrite II, la pyrite I est rare, remplacée partiellement ou complètement par la chalcopyrite et la pyrrhotite. Elle représente un vestige du premier assemblage paragénétique sulfureux du gisement (avec chalcopyrite et pyrrhotite en inclusions). L'or du gisement de Mouska présente une grande variété de formes. En terme de rapport Au:Ag, une nette distinction peut être constatée entre l'or en micro-inclusions dans la pyrite I (4 à 6% Ag) et l'or sous une autre forme (jusqu'à 25% Ag). Ce gisement diffère des gisements archéens de type veine de quartz par sa teneur élevée en sulfures dans les veines et par les caractéristiques des altérations associées aux zones de minerai. Les roches métabasiques sont associées à une auréole d'altération distale, et une autre proximale. Ces halos résultent d'une interaction progressive entre une empreinte hydrothermale prédeformation (événement sulfureux) et une autre tectonométamorphique (événement quartzique). Les études minéralogique, géochimique et isotopique montrent que les assemblages d'altération autour des zones de minerai varient non seulement avec la

§ *E-mail address*: abelkabir@fstg-marrakech.ac.ma

lithologie (basalte à andésite), mais elles indiquent aussi une histoire hydrothermale complexe. Les protolithes mafiques ont enregistré au cours de cette histoire plusieurs transformations en relation avec les dépositions de l'or avec sulfures et de l'or avec quartz. Dans les zones d'altération proximales, les bilans de masse révèlent une addition importante de K, reliée à l'enrichissement observé en biotite et en mica blanc en s'approchant des zones de minerai. Cependant, ces calculs n'affichent qu'une addition substantielle de SiO_2 dans les basaltes altérés, qui serait due à la destruction massive des minéraux ferromagnésiens, plutôt qu'à une addition hydrothermale de SiO_2.

Mots-clés: or, veines de quartz, veines de sulfures, altération hydrothermale, mine Mouska, ceinture de l'Abitibi, Québec.

Introduction

In an earlier paper (Belkabir & Hubert 1995), we examined the geometrical and structural aspects of the sulfide-rich Archean Mouska gold deposit, in the Abitibi Province of Quebec, with emphasis on interactions between host rocks, sulfide bodies, shear zones and quartz veins. The sulfide bodies were overprinted by ductile deformation, metamorphism and quartz veining. In the present paper, we provide mineralogical and geochemical data on the alteration of metabasic host-rocks and gold mineralization, and establish a paragenetic succession of this quartz–sulfide vein-type deposit. We also discuss the timing of gold introduction relative to the overall paragenesis. Furthermore, the whole-rock geochemistry, stable isotopes (S and O), and phyllosilicate compositions permit us to relate the observed alteration and mineralization to the composition of the fluids involved.

Background Information

The Mouska mine is located in the Bousquet mining district, in the southeastern part of the Archean Abitibi Greenstone Belt of the Superior Province (Fig. 1). The mine geology and ore mineralization were described in detail by Belkabir & Hubert (1995), and only a summary of these features is given here. The geology of the area is dominated by Archean bimodal mafic and felsic rocks of the Blake River Group. As a result of regional deformation, the volcanic units now trend east–west and have steep dips, with stratigraphic tops generally facing south. The regional planar tectonic fabric is vertical and also strikes east–west. Greenschist-facies metamorphism, accompanied by dynamic metamorphism (Vokes 1969), overprints all volcanic units.

The mineralization at Mouska is hosted by deformed basalts and andesites and coincides with shear zones (Fig. 1). The ore zones are composed of sulfide and quartz lodes; each ore zone differs from the others by its style of veining and by the nature of tectonism and metamorphism imprint. Gold is encountered in sulfides and quartz mineralization, as well as in adjacent altered host-rocks, and displays variable types of occurrences and habits, as described below. This study demonstrates that gold mineralization in the Bousquet metavolcanic rocks is early (*cf.* Marquis *et al.* 1990c). We also describe in detail the paths of hydrothermal–metamorphic alteration of the metabasic rocks at Bousquet, which are well exposed in the Mic-Mac and Mouska deposits. Recent preliminary work by Galley *et al.* (2003) on the Mooshla composite stock (Belkabir *et al.* 1998) suggests a genetic relationship between the mafic intrusive phases of the Mooshla, the metavolcanic rocks of the hanging wall and the stratabound sulfide mineralization of the Mouska and Mic-Mac deposits. This conclusion confirms the main role of the hydrothermal–syngenetic event on the deposition of gold and sulfides in the Bousquet district.

Mineralization

Distribution and styles

Economic gold mineralization at Mouska is confined to three ore zones (07, 08 and 22) hosted by a single shear system and forming three separate orebodies (Fig. 1). Zones 07 and 08 are characterized by quartz–sulfide and quartz-dominant veins, both hosted by andesitic units, whereas zone 22 is distinguished essentially by sulfide-dominant mineralization in the form of sulfide stringers associated with minor quartz veins and hosted by magnetic basalt (a first MAG-geophysical target). Therefore, gold ores can be classified as being gold–sulfide– and gold–quartz-dominant on the basis of the relative abundance of sulfides and quartz in veins. Gold–sulfide and gold–quartz mineralization types have similar simple assemblages of ore and gangue (Table 1). They are composed principally of pyrrhotite and chalcopyrite, together with minor amounts of pyrite and variable amounts of magnetite and ilmenite. It is evident though that gold–quartz mineralization is multistage; it is syn- to late-tectonic and displays progressive shearing and remobilization of pretectonic Au–sulfide ore, as is typical of many syntectonic vein-hosted gold deposits in the Abitibi mining district.

Mineralogy and textures

Pyrrhotite and chalcopyrite are the dominant sulfides (Table 1). In sulfide veins, both pyrrhotite and chalcopyrite exhibit smooth, arcuate mutual replacement and intergrowth textures (Fig. 2a) suggesting a stable paragenetic association of these minerals (Stanton 1972, Nguyen *et al.* 1988). However, chemical etching of vein sulfides in polished sections (using 25% HNO_3, fol-

lowed by a brief exposure to 20% HCl) reveals several features and microfabrics typical of dynamic metamorphism (Rickard & Zweifel 1975, Vokes 1969, Frater 1984). Chalcopyrite grains are elongate and foliated (Fig. 2b), but exhibit a granoblastic polygonal texture. During deformation, chalcopyrite generally deforms in a ductile manner and recrystallizes to a greater degree than pyrrhotite, filling fractures and low-pressure shadow zones (Vokes 1969). Pyrrhotite and chalcopyrite show evidence of many generations. They are also encountered as small inclusions (<20 μm) in fine-grained pyrite (Fig. 3c). These inclusions are generally not oriented, excluding any control by the pyrite host over their distribution.

Unlike sulfide veins, the quartz veins host pyrrhotite and chalcopyrite that exhibit a relatively weak state of strain. In this case, the deformation of sulfides is characterized by fracturing and brecciation of grains, and rarely by textures that would suggest softening and high ductility. Pyrrhotite is also located in magnetite porphyroblasts (Fig. 4b).

Pyrite is generally present as a minor component of the sulfide veins (<5%), but in disseminated sulfide stringers (zone 22), its abundance is similar to that of

TABLE 1. MINERALOGY OF VEIN MATERIALS AT THE MOUSKA DEPOSIT, BOUSQUET DISTRICT, ABITIBI GREENSTONE BELT, QUEBEC

	n	Po	Cp	Py	Mgt	Ilm	Hem	Sil	Assemblage
Ore zone 07									
Sulfide vein	8	50	25	5	8	3	1	7	qtz-chl-bt-cal-ep-rt
Quartz vein	10	7	10	2	3	2	Tr-1	76	qtz-ab-bt-cal-ap-ep-chl
Ore zone 08									
Sulfide vein	7	45	25	6	5	2	2	15	qtz-chl-bt-cal-ep-rt
Quartz vein	4	4	7	4	2	2	1	80	qtz-chl-bt-cal-ep-ms
Ore zone 22									
Disseminated stringers	13	3	2	1	8	4	2	80	qtz-chl-bt-cal-ep-ms-rt

Mineral proportions are reported in volume %; *n*: number of samples studied.

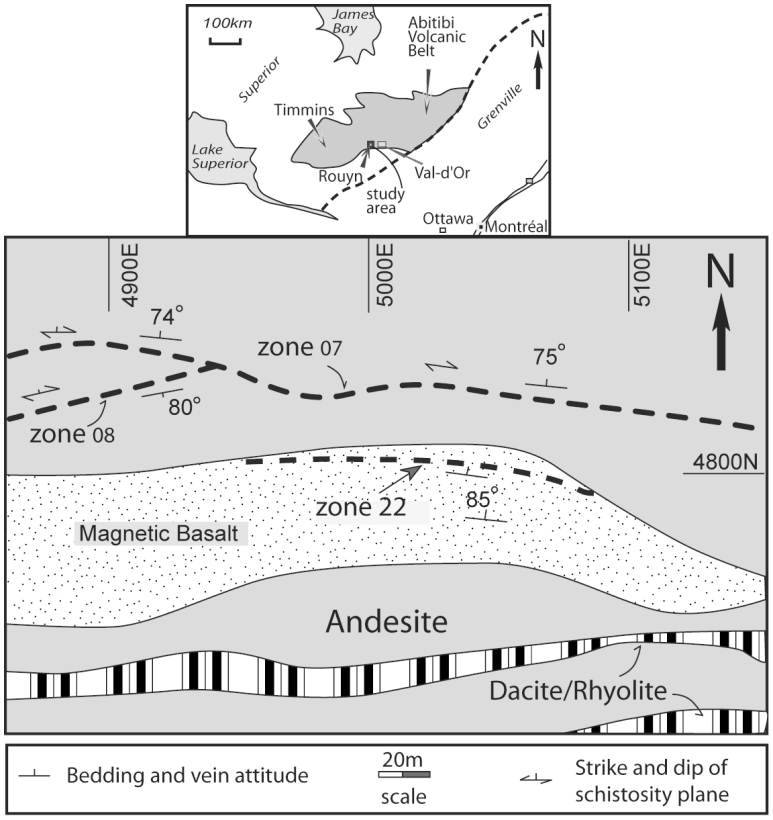

FIG. 1. Simplified geological map of the Mouska deposit at mine level –200 m.

pyrrhotite or chalcopyrite (Table 1). On the basis of grain size and textural relationships, we recognize two types of pyrite. The earlier one (pyrite I) is fine grained (ë0.1 mm) and generally occurs as disseminations of anhedral aggregates (Fig. 2c); it is confined to the gold–sulfide mineralization and exhibits textures typical of metamorphosed massive sulfide ore (Vokes 1969), such as rounded grains and embayment textures of the "caries type" (Fig. 2d). As shown in Figures 2c and 2d, this pyrite, embedded in sulfide lenses, is not severely

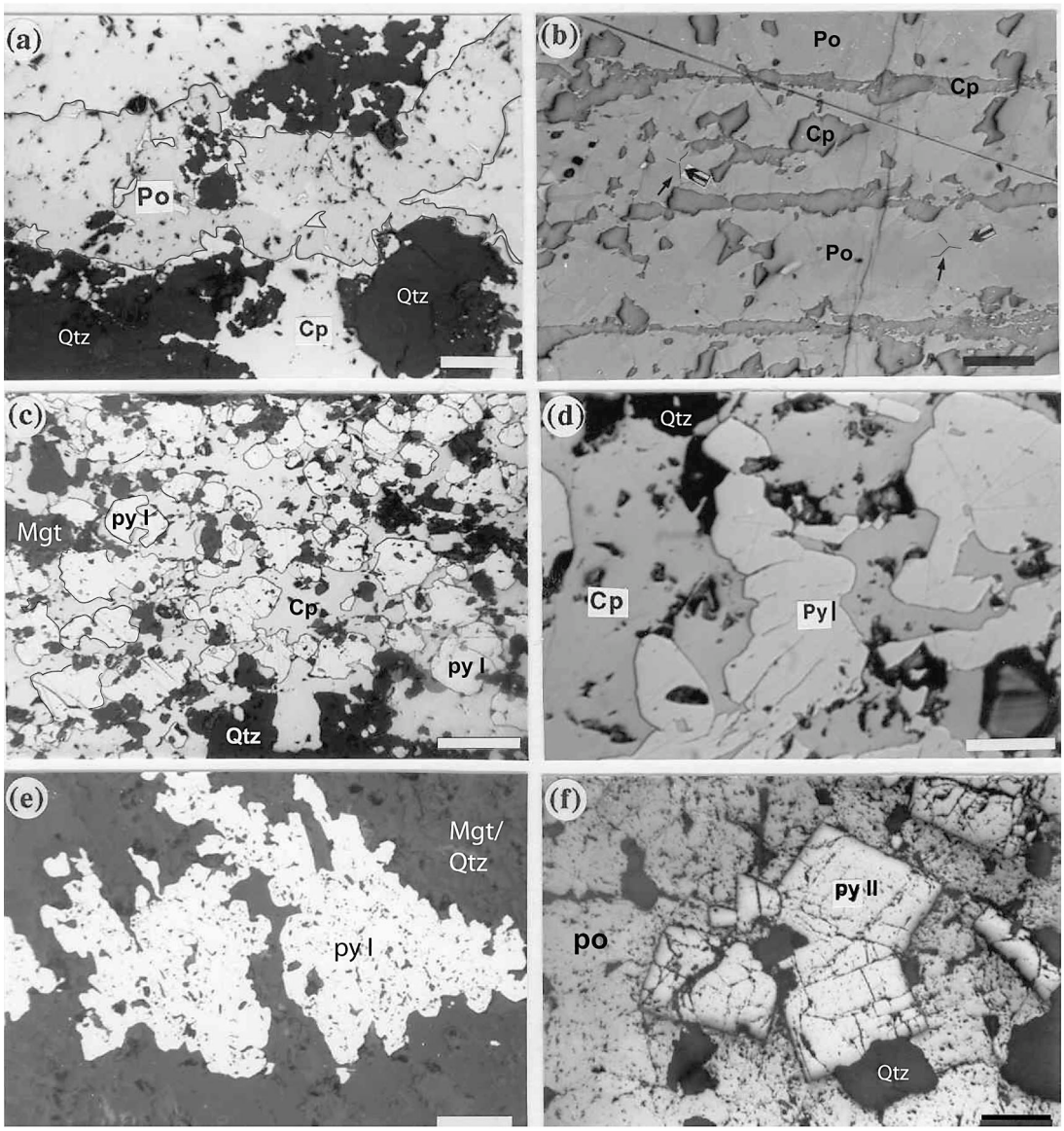

FIG. 2. (a) Pyrrhotite (po) and chalcopyrite (cp) intergrowths or replacement texture; chalcopyrite (cp) fills embayments and fractures in pyrrhotite (po) in a massive sulfide vein (scale is 0.2 mm). (b) Granoblastic texture with 120° triple junction (foam texture) in metamorphosed chalcopyrite-rich ore (see arrows) (scale is 0.2 mm). (c) Fine-grained pyrite embedded in lens of chalcopyrite–pyrrhotite (scale is 0.1 mm). (d) Corroded early fine-grained pyrite I (pyI) in sulfide veins, with ragged edges in pyrrhotite–chalcopyrite matrix (scale is 0.04 mm). (e) Fine-grained pyrite I, altered to magnetite (mgt) and deformed in disseminated ore (scale is 0.04 mm). (f) Late pyrite (py II) grains showing irregular arrays of fractures (scale is 0.4 mm).

strained, the strain having being taken up by the ductile pyrrhotite–chalcopyrite matrix. On the other hand, grains of pyrite I in disseminated ore are sheared parallel to tectonic fabrics (Fig. 2e). In rare cases, the pyrite I is associated with small (20 to 60 μm) idiomorphic grains of arsenopyrite. The latter occurs at the margins of pyritic bodies and is generally not observed elsewhere in the ore zones at Mouska.

The second pyrite (type II) is typically coarse grained (0.5 to 3 mm) and appears as idiomorphic grains and aggregates within the gold–sulfide and gold–quartz veins, as well as in the surrounding host-rocks (Fig. 2f). Although it is locally fractured, it is chiefly late tectonic or, in very rare cases, later than the foliation and cross-cuts it. Most of the inclusions encountered within pyrite II are composed of silicates, carbonates and hematite;

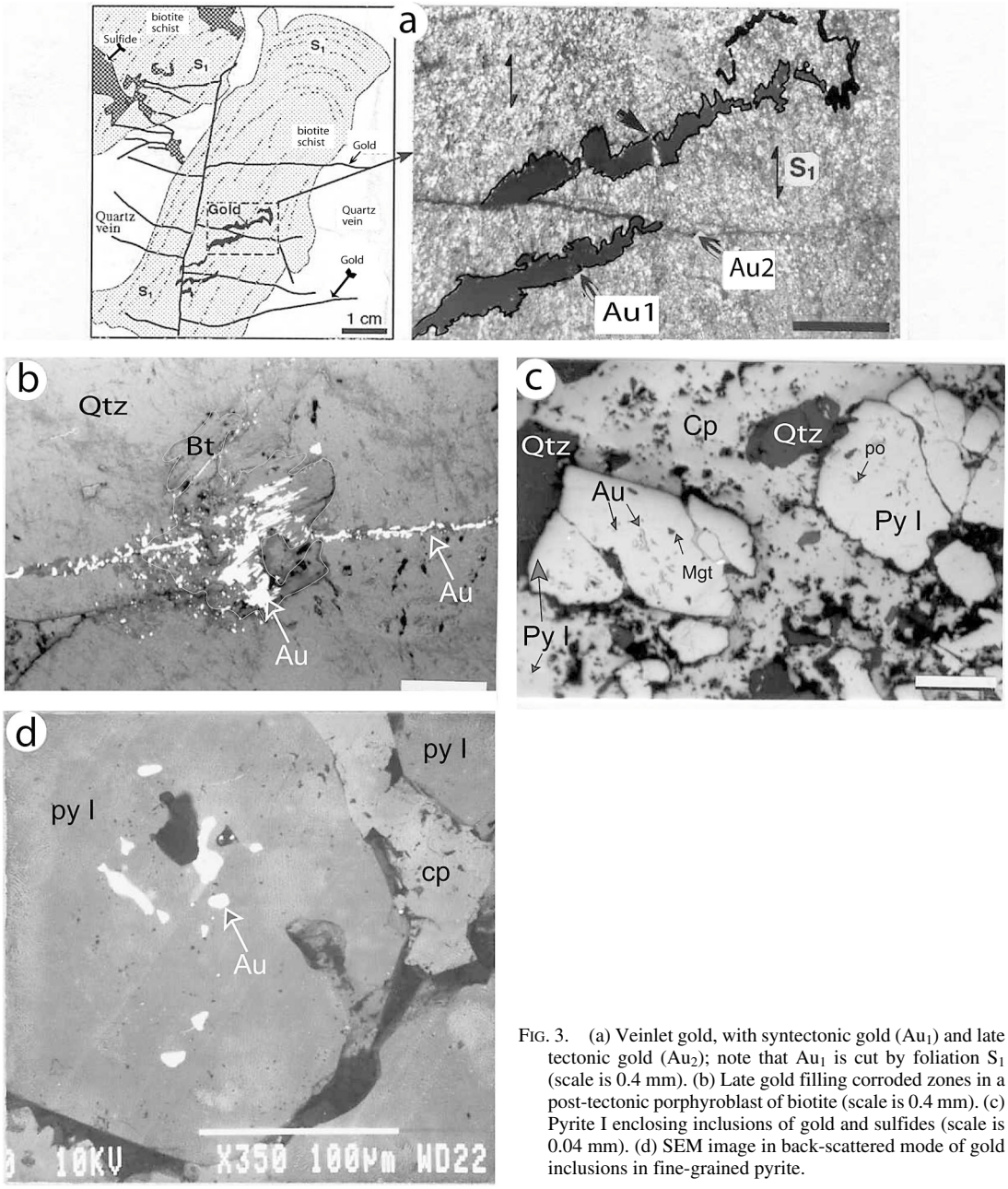

FIG. 3. (a) Veinlet gold, with syntectonic gold (Au_1) and late tectonic gold (Au_2); note that Au_1 is cut by foliation S_1 (scale is 0.4 mm). (b) Late gold filling corroded zones in a post-tectonic porphyroblast of biotite (scale is 0.4 mm). (c) Pyrite I enclosing inclusions of gold and sulfides (scale is 0.04 mm). (d) SEM image in back-scattered mode of gold inclusions in fine-grained pyrite.

neither gold or other sulfide inclusions are present in grains of pyrite II.

Throughout the ore zones 07, 08 and 22, gold exhibits a wide range of occurrences and habits, and commonly appears as visible gold, in veins as well as in the host rocks. It generally occurs as free grains (up to 5 mm) or as clouds of very fine grains, particularly in the silicate gangue. Gold fills minute fractures (veinlets) in quartz or in the sulfide veins, as well as in the host rocks. The veinlets can be either syntectonic (deformed and transposed parallel to tectonic fabrics) or late tectonic (undeformed and cross-cutting S_1) (Fig. 3a). In some cases, veinlets of gold are injected across post-deformation porphyroblasts of biotite or chlorite (Fig. 3b). This gold is probably related to late hydraulic fracturing or to a later event of stress relaxation.

Gold also is found as minute inclusions (5 to 10 μm) in fine-grained pyrite I, forming irregular aggregates or grains on its surface. These inclusions are randomly distributed and do not show any preferred orientation (Fig. 3c). In the sulfide veins, gold in pyrite I has been examined by scanning electron microscopy (SEM) as well as in back-scattered electron mode (BSE–SEM); these photomicrographs show that most of the gold, as well as the associated chalcopyrite and pyrrhotite inclusions, are unrelated to pyrite structure or fracture fillings (Fig. 3d) in the prominently homogeneous host pyrite I.

Magnetite, ilmenite and minor amounts of hematite and rutile are the principal Fe–Ti oxide minerals identified at Mouska. Generally, they represent a minor component of the ore minerals, not only in vein material, but also throughout the surrounding rocks, except in the case of the disseminated sulfide stringers, where magnetite is abundant (Table 1). As mentioned above, ore zone 22 coincides with a band of magnetite-rich basalt, well outlined on magnetic geophysical maps and sections. Magnetite appears as deformed and elongate grains or aggregates oriented parallel to tectonic fabrics (Fig. 4a) or as large scattered euhedral to subhedral porphyroblasts (Fig. 4b) included in and with inclusions of pyrrhotite. Several modes of occurrence were recorded for porphyroblastic magnetite: (1) magnetite partly or wholly embedded in lenses of pyrrhotite–chalcopyrite, (2) magnetite within fracture-fillings of quartz–calcite and sulfides (Fig. 4b), and (3) magnetite containing inclusions of quartz, calcite and pyrrhotite. This latter case is mostly pyrrhotite and interpreted as the precursor of magnetite.

Ilmenite is present in small but consistent amounts in veins and can be either metamorphic or hydrothermal, occurring as small (30 to 40 μm) platy crystals replacing deformed grains or veinlets of magnetite. Locally, ilmenite was affected either by late fluids (as shown by rims of titanite) or by minor cataclastic deformation, as indicated by the presence of internal cracks.

Hematite and rutile are also present in small amounts as idiomorphic grains (50 to 80 μm) generally replacing magnetite. In a few cases, these oxides are observed as isolated porphyroblasts associated with quartz, white mica, biotite, and calcite dominantly.

Silicate minerals, the main component of the gangue in the gold-bearing veins, correspond to a wide range of low-grade metamorphic minerals (Table 1). In gold-dominant sulfide mineralization, the silicates are principally in the quartz – calcite – epidote association, hosted by the chalcopyrite–pyrrhotite matrix. Quartz and calcite are recrystallized and coarse grained. Like the fine-grained pyrite, the competent quartz–calcite assemblage was also protected from deformation by the surrounding ductile sulfides. Epidote occurs as large (up to 1 mm), locally fractured and weakly strained, isolated, idiomorphic grains. Thus, the silicates within the undeformed fragments incorporated inside a massive sulfide are represented by the assemblage quartz – calcite – chlorite – biotite – epidote. In quartz veins, the predominant silicate is quartz itself, generally accom-

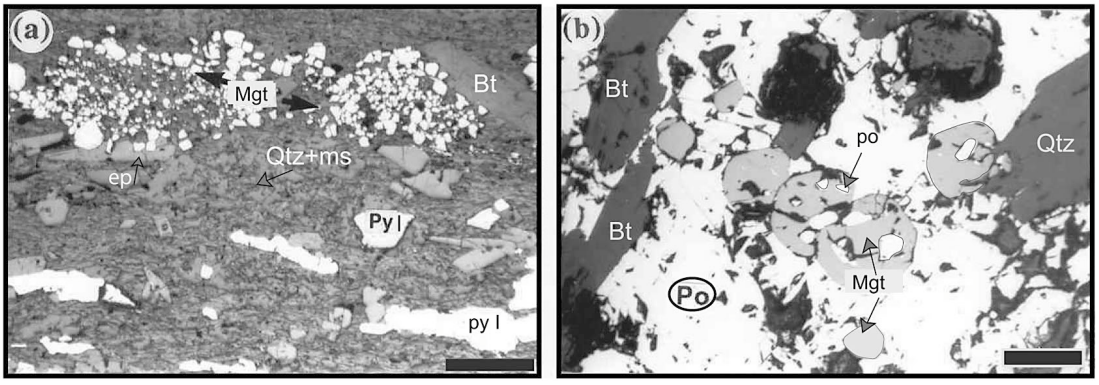

FIG. 4. (a) Deformed aggregates of magnetite (mgt) grains parallel to foliation and to pyrite 1 (PyI) (scale is 0.1 mm). (b) Magnetite porphyroblasts with inclusions of pyrrhotite (Po), and included in pyrrhotite matrix (scale is 0.1 mm).

panied by other syn- to late-tectonic chlorite and biotite (Table 1). These syntectonic minerals are strongly strained and oriented parallel to foliation, whereas post-tectonic minerals (such as biotite, chlorite and epidote) were clearly formed subsequent to foliation.

Geochemical Relationships

Chemical compositions of gold particles at Mouska provide important information about the succession of ore minerals and genetic relationships between gold and host minerals. The compositions of gold grains from several occurrences and habits were established using the McGill University JEOL JXA–8900L Super Probe, operated at 20 kV with a sample current of 30 nA. From the results of 140 analyses, a compositional trend of Ag–Au alloy was established (Fig. 5). Composition A, clustering around 96 wt.% Au and 4% Ag, comprises gold occurring as micro-inclusions in fine-grained pyrite I. Composition B, clustering around 90% Au and 10% Ag, pertains to free gold or veinlet gold. Composition B', clustering around 85% Au and 13% Ag, and composition B", clustering around 75 wt.% Au and 22% Ag, characterize some large grains of free gold and late gold in fracture fillings that cross-cut the foliation (*e.g.,* Fig. 3a). Populations B, B'and B'' form a continuum of Au:Ag values, suggesting a genetic interrelationship. Selected grains representing the three Au:Ag populations were also analyzed for Fe, Cu, Pb, Sb, Bi, As and Hg (Table 2a). In all cases, As, Bi and Sb occur in insignificant amounts, whereas Cu, Pb, Hg and Fe are readily detected and show wide compositional variations. Among the 36 analyses performed, Fe is consistently higher in micro-inclusions of gold (A) compared to the other two modes of occurrences (B, B' and B"); this association is also reflected to a lesser extent by Cu (Table 2a). The higher Fe values in the gold inclusions may also be due to the possible Fe contamination from the host pyrite I.

The pyrite I was also analyzed for Fe, Cu, Pb, Au, Ag, Bi, Te and S using the elecron microprobe. Lead and Te are undetectable in the pyrite grains analyzed. Trace gold in pyrite grains was mostly below the detection limit (<140 ppm) (Table 2b). Elevated concentrations of Au in pyrite I are directly related to the gold as inclusions, suggesting that pyrite I and gold were clearly related genetically. In an earlier report on the composition of gold at Mouska, Wilhelmey (1987) separated and analyzed (by ICP–MS) several fractions of ore (pyrite, pyrrhotite and chalcopyrite) for gold. He noted firstly the presence of the fine-grained pyrite in the fine fractions of ore (<100 μm), and secondly the significant high amounts of gold (up to 1560 ppm) in the analyzed mineral-fractions (pyrite I). He also analyzed 30 grains of gold, varying from coarse (*e.g.,* free gold outside pyrite I) to fine grained (<10 μm; gold in pyrite I), and concluded that the coarser gold, unlike the fine grains, commonly contains significant amounts of Ag (17 to 19 wt.%), Bi (800–1200 ppm) and Pb (500 to 550 ppm).

Hand specimens of quartz and sulfide veins have been also analyzed by ICP–MS for Au, Ag, Cu, Pb, Zn, Co, Ni and V. In Table 2c, we show that pyrite in sulfide-rich veins is significantly more enriched in Co, Zn and Ni than in quartz-rich veins. On the other hand, the Cu contents are variably enriched, probably reflecting the presence of chalcopyrite in both types of mineralization.

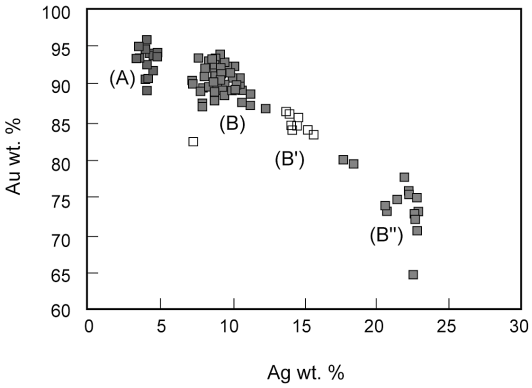

FIG. 5. Gold *versus* silver plot of results of 140 electron-microprobe analyses of 37 gold grains as (A) micro-inclusions in fine-grained pyrite; (B) stringers or isolated grains in sulfide and quartz veins.

TABLE 2a. CHEMICAL COMPOSITION OF GOLD GRAINS, MOUSKA DEPOSIT,BOUSQUET DISTRICT, ABITIBI GREENSTONE BELT, QUEBEC

	n	Au	Ag	Cu	Pb	Hg	Fe	Total
gold (A)	14	93.2	4.2	0.1	0.2	0.2	1	98.8
gold (B)	15	88	9.4	0.1	0.2	0.2	0.5	98.3
gold (B'')	8	73.5	21.8	1.1	0.4	0.2	0.4	97.31

Chemical composition, reported in wt.%, is an average result of *n* analyses. Gold (A) is present as inclusions in fine-grained pyrite I; (B) and (B") represent gold grains in other occurrences. See Figures 3 and 5.

TABLE 2b. CHEMICAL COMPOSITION OF FINE-GRAINED PYRITE IN GOLD ORE, MOUSKA DEPOSIT, BOUSQUET DISTRICT, ABITIBI GREENSTONE BELT, QUEBEC

Sample	*n*	Au	Ag	Fe	Cu	Bi	S
2890	5	<140	<170	46.7	0.1	0.1	53.5
M4	9	250	<170	46.6	0.2	0.1	53.1
M3	9	<140	<170	46.4	0.1	0.1	53.1
2878	6	<140	<170	46.9	0.1	0.1	53.4

Concentrations of Fe, Cu, Bi and S are expressed in wt.%; those of Au and Ag are expressed in ppm. These are the results of *n* analyses.

Selected specimens of ore were studied in more detail, firstly by separating gangue minerals from sulfides, and secondly, by distinguishing between magnetic (pyrrhotite-rich) and non-magnetic ore (chalcopyrite–pyrite-rich). Several points can be deduced from these data. In twelve samples of vein gold (gangue and ore) from the types of gold mineralization described above, silicate gangue constitutes approximately 38%, the pyrrhotite-rich fraction 6%, and the pyrite–chalcopyrite-rich fraction 56%. In samples where pyrite is a major component of the ore fraction, the gold content is markedly higher in the nonmagnetic fraction (Table 2d). The higher content of gold in the nonmagnetic fraction is due to the higher chalcopyrite content, as indicated by elevated Cu values, and, to a lesser extent, the presence of the auriferous pyrite I.

Paragenesis

Gold mineralization at Mouska occurred during several stages of deposition, ranging from a predeformation sulfide-dominant stage to a multistage quartz-dominant syndeformation stage. Textural relationships among ore minerals (see above), combined with results of prior structural analyses (Belkabir & Hubert 1995), indicate that progressive shearing occurred after the formation of a first generation of ore minerals, including pyrite I, chalcopyrite, pyrrhotite, magnetite and gold, all of which are confined to an early stage of gold–sulfide mineralization. Among these minerals, only the preexisting pyrrhotite – chalcopyrite – gold assemblage in pyrite I belongs to the early-stage mineralization. In sulfide veins, the embedding of pyrite I aggregates in the metamorphosed and deformed pyrrhotite–chalcopyrite assemblage and the local preservation of this pyrite I from deformation confirm the early pyritization event. The main predeformation events documented in the Bousquet district were volcanism, giving the Blake River Group, and the earlier deposition of sulfides (Tourigny *et al.* 1988, 1993, Marquis *et al.* 1990a, b, Belkabir & Hubert 1995). At the Mouska deposit, this early stage is assumed to result in pyrite-rich ore (pyrite I) and sulfides. Textural relationships indicate destabilization [*e.g.,* increase $f(S_2)$] and transformation (replacement) of the more iron-rich sulfides (pyrrhotite–chalcopyrite matrix) to form pyrite I. During the multistage quartz mineralization, a part, if not all, of the sulfide may have resulted from short-range remobilization and recrystallization of earlier sulfides (Belkabir & Hubert 1995). In Figure 6, we summarize the above-mentioned paragenetic successions at Mouska.

Wallrock Alteration

Petrography and distribution of altered metabasic rocks

The mineral assemblages of the least-altered metabasic rocks, containing albite or oligoclase, altered hornblende, chlorite, epidote, quartz and calcite, together with minor amounts of biotite, white mica and oxides, are typical of greenschist-grade conditions. However, the southernmost basaltic lithologies, as well as the proximal andesites, are markedly silicified near the many felsic units. Outside the shear zones, silica enrichment is found as centimeter-scale layers of chert along minor faults as well as a silicification of pillow rims. Regional metamorphism in the undeformed metabasic rocks has generally preserved the original textures (Figs. 7a, b). The prograde metamorphism accompanying the development of the S_1 schistosity ($\approx S_2$ regional schistosity) in the metabasic rocks of the Bousquet area is known to have reached the greenschist–amphibolite transition, with calculated temperatures of 440 ± 25°C and pressures of 2.0 to 3.8 kbar (Stone 1988, Marquis *et al.* 1990a).

In Figure 8, we summarize the relative distribution of alteration zones and their mineralogical characteristics throughout the deposit. Lithological units are sche-

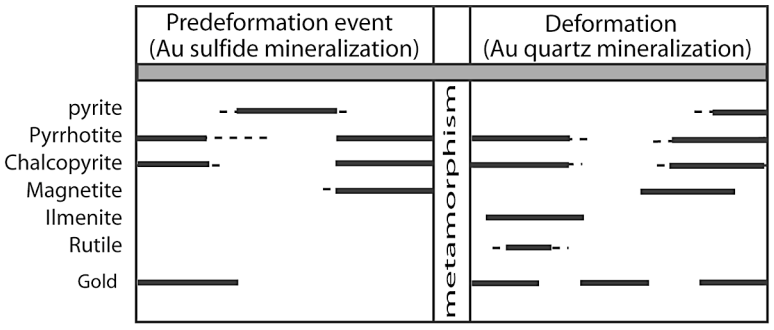

FIG. 6. Schematic paragenetic sequence for pre- and syndeformational gold mineralization at Mouska. See text for explanation.

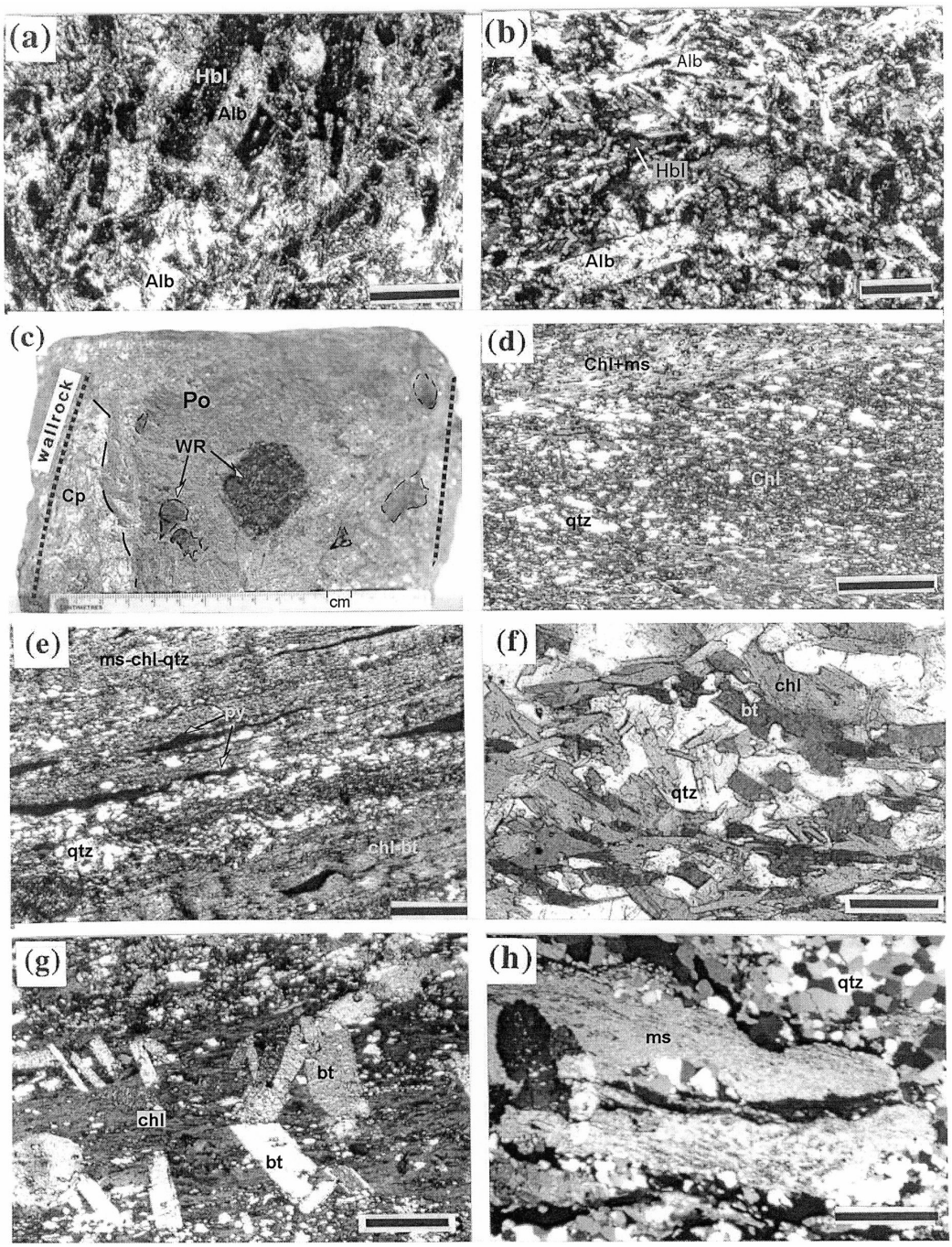

FIG. 7. (a) and (b) Photomicrographs showing, respectively, a least-deformed medium-grained meta-andesite and a least-deformed meta-basalt with fine-grained laths of albite (scale bars are 0.5 and 0.2 mm). (c) Angular fragments of undeformed wallrock (WR) incorporated inside a massive sulfide vein (up to 85% sulfides). (d) Chlorite schist in andesitic unit (scale bar is 0.5 mm). (e) Chlorite schist in basaltic unit showing deformed grains of magnetite parallel to the main foliation (scale bar is 0.5 mm). (f) Biotite schist, with biotite is partly retrograded to chlorite (scale bar is 0.5 mm). (g) and (h) Host schist of disseminated ore in zone 22 showing, respectively, the mafic layers composed of chlorite with post-tectonic biotite and felsic layers dominated by white mica – quartz assemblage.

matically represented, as they vary notably in width and vertical extent.

Although Belkabir & Hubert (1995) clearly demonstrated that sulfide mineralization took place prior to dynamic metamorphism, the timing of the hydrothermal alteration accompanying emplacement of the sulfides is not easily identified, because this alteration has been obliterated to variable degrees by later deformation and metamorphic events. In the 08 and 07 ore zones, altered fragments of breccia lacking foliation within a dominantly biotite – quartz – epidote assemblage and enclosed by deformed sulfide veins suggest a pre-dynamic metamorphic alteration (Fig. 7c). The breccia fragments were apparently incorporated in the sulfides during their original formation and were further shielded from deformation by their rheological contrast with their host sulfides.

Two alteration assemblages are recognized in altered metabasic rocks, both followed by a progressive destruction of the original textures and a gradual develop-

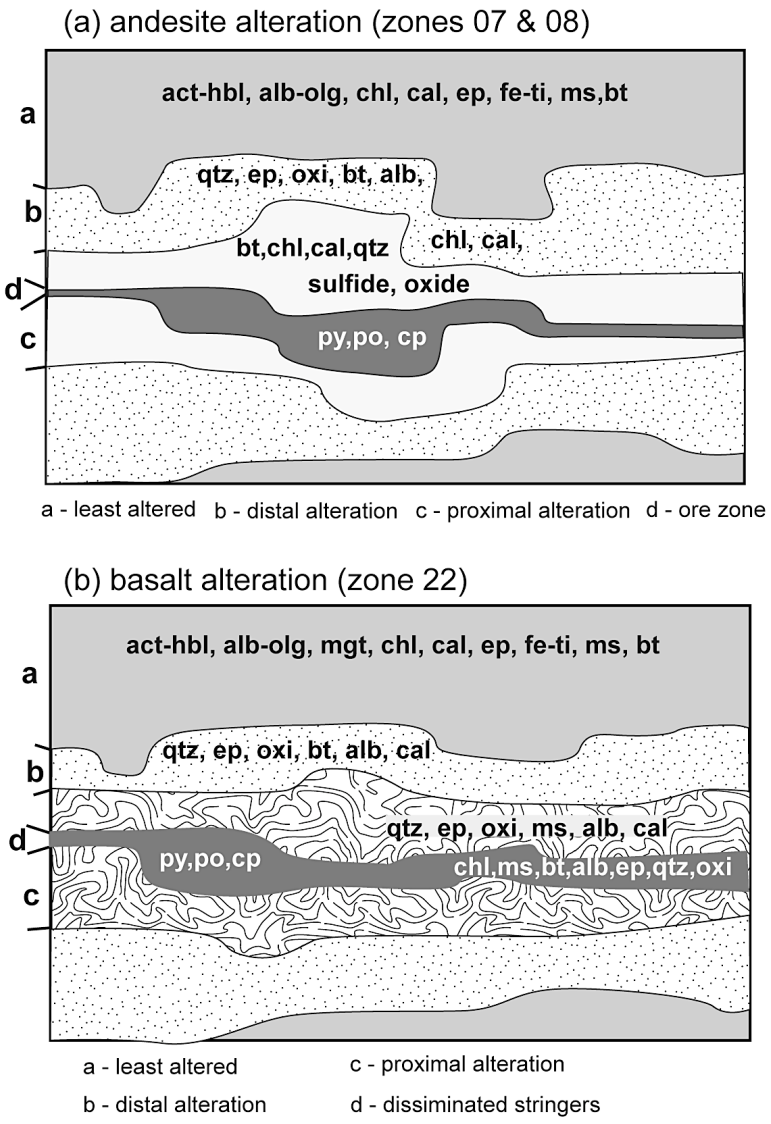

FIG. 8. Schematic distribution of ore and alteration zones in (a) andesite and (b) basalt facies.

ment of penetrative deformation. The distal alteration, marked by a chlorite zone and characterized by modal amounts of dark green to gray-green chlorite after hornblende and actinolite, is associated with a calcite – epidote – quartz assemblage, as well as minor amounts of albite, biotite, pyrrhotite and ilmenite (Figs. 7d, e). In altered metabasic rocks, the chlorite zone is pervasively developed over large areas in which chlorite forms thick (~1 mm) crenulated mafic laminations intercalated with quartz and calcite. In these laminations, magnetite and ilmenite, representing a distinct enrichment in iron oxides, are generally deformed and stretched parallel to the main foliation (Fig. 7e). In andesites, the chlorite zone is characterized by deformed aggregates of fine-grained chlorite partly replaced by quartz and calcite (Fig. 7d).

The proximal alteration (basalt and andesite) bordering the ore zones is outlined by a potassium-rich halo in which biotite occurs as slightly deformed syntectonic and undeformed post-tectonic porphyroblasts. These biotite zones are generally narrow and restricted compared to the distal zones of alteration. In andesite, the proximal alteration is simple and characterized by a schistose biotite – chlorite – calcite – quartz assemblage, with minor amounts of albite, sulfides (pyrrhotite, chalcopyrite and pyrite) and iron oxides (magnetite and ilmenite). Biotite is partly retrograded to chlorite and quartz. In basaltic lithologies, the proximal zone is more complex, as it is not gradually changed toward the ore zones but displays many segregated phyllosilicates and centimetric quartz-rich layers. At their distal ends, the biotite zones are analogous to those in the andesites and are characterized by intense formation of biotite in the schist. Within the mineralized ore zones, the proximal alteration displays a clear enrichment of quartz and white mica associated with the chlorite – biotite – calcite – albite assemblage. The host schist of disseminated ore in zone 22 is composed of intercalated leucocratic and melanocratic laminations characterized, respectively, by dominant quartz – white mica – calcite (Fig. 7f) and chlorite–biotite-rich assemblages (Fig. 7g). In this ore zone, post-tectonic porphyroblasts of biotite are prominent and are generally retrograded to quartz, chlorite and white mica (Fig. 7h). An increase in modal quartz accounts for the many centimeter-thick deformed units of interflow chert, as well as locally apparent silicification of the schist. At the mesoscopic scale, the silicification is non-pervasive, being sparsely distributed throughout the schist. This silicification increased the rigidity of the schist such that, megascopically, it seems nearly undeformed.

The proximal and distal zones of alteration developed by progressive interaction with a single metamorphic fluid. This conclusion is based on the observations that: 1) the alteration zones surround the ore zones, 2) the thickness of the distal zones of alteration is consistently greater than that of the proximal zones of alteration, 3) zones displaying assemblages of proximal alteration have not been observed in direct contact with unaltered metabasic rocks, and 4) mineralogical changes in both proximal and distal zones of alteration are similar, essentially differing only in the abundances of the metamorphic minerals.

Chemical changes during hydrothermal alteration

Undeformed samples, having distal and proximal alteration-induced assemblages and ranging from andesitic to basaltic compositions, have been analyzed for major and selected trace elements by X-ray-fluorescence spectrometry at the McGill University Geochemical Laboratory (Table 3). Most of the least-altered metamorphosed mafic rocks plotted on a Floyd & Winchester (1978) diagram fall within the basalt and andesite fields. The more altered samples are outlined by increases in alkali and silica contents. On an AFM diagram, the least-altered samples plot chiefly in the tholeiite field or near the tholeiitic – calc-alkaline boundary in the case of more altered samples. Flat rare-earth-element patterns (La/Yb_n in the range 0.8 to 1.9) confirm the tholeiitic affinity of these volcanic rocks. The basalts are slightly more enriched in rare-earth elements than the andesites.

To examine the nature of the alteration, the gains and losses of chemical components have been determined for least-altered samples of metabasic rocks and compared to those in zones of proximal alteration. Calculated mass-balances have been related to observed mineralogical changes. The isocon approach of Grant (1986) has been applied to express the flux of components as gains (positive) or losses (negative) from the least-altered to the more-altered rocks. The selection of the isocon for each case is based on the best-fit line for normally immobile components such as Ti, Zr, Nb, Y and Al. Most of these components, plotted one against another, produce a linear plot that passes through the origin (*cf.* MacLean & Kranidiotis 1987). Their immobilities have been tested from correlation coefficients for regression lines, and the most immobile pairs of elements have been selected.

In the ore zone 07, the isocon coincides well with the best-fit line that passes through the origin and the most immobile elements (Fig. 9a). From the respective density of least-altered and altered rocks, a loss of volume of 13% is evident (isocon slope m = 1.15), which can be considered to be within an acceptable range of geological variability for this ore zone. In the case of the ore zone 22, the isocon passes close to some immobile elements (Y, Nb, Al, Zr and Ti), but is closest to the $Zr–TiO_2$ pair (Fig. 9b). The change of volume corresponding to this isocon (slope m = 1.3) represents a volume loss of up to –18% and up to –45% in the host schist of the disseminated ore.

For andesitic rocks (Fig. 9a), mass-balance calculations of proximal alteration relative to the least-altered andesite indicate marked enrichments in K, Rb and Ba.

In contrast, Si, Al, Mg, Mn, Fe and Ca are slightly depleted or in the normal range of variability. Gains in K account for the formation of biotite, which clearly characterizes the proximal alteration. For the ore zone 22, mass-balance calculations of proximal alteration relative to the least-altered basalt (Fig. 9b) show that K, Na, $Fe_{(total)}$, Ba and Rb have been added in the altered rocks, and Ca, Mg, Mn, Nb and Sr were depleted. Magnesium has been removed from the rocks during replacement of the mafic minerals biotite and chlorite by white mica and quartz. The chemical behavior of Si (slightly modified or unaffected) does not coincide with the apparent silicification of the altered metabasalts, particularly in the host schist of disseminated ore in zone 22. Thus, we

TABLE 3. BASALT AND ANDESITE COMPOSITIONS FROM THE MOUSKA DEPOSIT, BOUSQUET DISTRICT, ABITIBI GREENSTONE BELT, QUEBEC

Sample	SiO_2	Al_2O_3	Fe_2O_3	MgO	CaO	Na_2O	K_2O	TiO_2	P_2O_5	MnO	LOI	Total	Nb	Zr	Y	Sr	Rb
andesite																	
2897	44.48	12.94	12.74	7.77	8.4	1.96	0.23	1.09	0.08	0.18	5.58	95.45	5.7	78	29	73	7.6
2956	51.56	17.27	9.98	4.94	7.77	4.81	0.3	0.83	0.09	0.11	2.19	99.85	4.8	71	13	138	4.5
2967	44.1	7.11	3.41	0.01	27.71	0.33	0.07	0.26	0.03	0.16	16.31	99.49	3.8	31.2	21.8	149.1	3.6
2969	52.56	13.39	13.67	5.67	9.78	2.71	0.2	1.02	0.07	0.18	1.21	100.46	7	104.7	38.7	99.5	3.8
2876	50.78	13.1	11.35	7.98	10.32	1.63	0.13	0.89	0.07	0.17	2.83	99.25	5.7	86	30	203	4.5
1321	49.26	12.36	22.87	3.44	1.18	2.5	0.52	2	0.2	0.08	6.22	100.63	8.7	110	50	44	15
1383	49.11	15.71	10.1	5.53	8.53	3.3	0.18	0.82	0.1	0.16	6.32	99.86	5.7	81	17	93	4.5
1385a	48.3	12.32	12.25	7.12	11.26	0.98	0.06	0.87	0.07	0.19	5.69	99.11	4.8	78	30	82	1.5
1409	56.63	14.64	11.07	4.65	3.19	3.21	1.26	1.05	0.14	0.08	3.65	99.57	6.7	88	26	92	34
1425	58.88	13.87	12.64	2.17	1.45	0.74	3.71	2	0.1	0.1	3.86	99.52	12	138	75	18	102
2882a	45.22	16.79	18.21	5.38	3.39	3.04	3.86	0.94	0.08	0.1	1.46	98.47	5.5	59	8.8	80	162
2892	52.87	13.15	18.55	5.88	2.72	1.61	0.34	1.1	0.1	0.17	3.78	100.27	7.7	118.2	43.2	36.4	10.6
2893	46.37	11.57	13.82	4.79	9.46	2.78	1.41	0.89	0.07	0.17	6.18	97.51	6.7	90	32	45	54
2895	42.96	11.68	12.87	5.8	11.58	1.97	1.94	0.93	0.06	0.21	9.66	99.66	4.3	61	26	74	64
2896	44.45	12.75	11.94	5.59	10.92	2.86	0.04	1.03	0.07	0.24	9.32	99.21	5.5	76.9	31.7	86	1.7
2898	51.4	13.2	12.1	8.15	8.4	0.98	0.11	0.94	0.08	0.18	3.05	98.59	15	76	28	71	12
1351	47.6	13	14	5.68	10.2	1.23	0.19	1.48	0.12	0.2	5.8	99.5	15	63	18	142	13
1352	45.8	11.3	10.3	7.5	11.4	1.13	0.39	0.7	0.06	0.2	11	99.78	13	61	18	96	19
1353	49.4	12.9	11	6.44	9.33	1.72	0.01	0.97	0.08	0.19	7.05	99.08	24	72	26	97	13
1354	55.4	8.31	23.4	3.23	1	1.33	2	0.72	0.06	0.08	3.55	99.08	32	70	17	15	61
1355	48.8	12.5	10.9	6.07	8.93	2.24	0.41	1	0.08	0.17	7.75	98.85	16	96	19	79	12
2887b	47.5	15.1	11.3	9.33	11	1.31	0.25	0.64	0.04	0.19	2.2	98.86	27	33	10	55	10
2887c	51.6	14.4	10.9	7.17	9.13	1.69	0.2	0.87	0.07	0.15	2.55	98.73	17	73	31	290	10
2959	49.51	14.79	11.25	7.53	9.71	1.76	0.19	0.86	0.06	0.15	2.86	98.67	6.1	89	32	296	5.3
2973	54.56	13.11	18.56	1.87	3.17	5.18	0.1	1.91	0.28	0.04	1.25	100.03	11	178	66	94	5.8
1334	51.37	15.46	8.7	0.82	9.71	5.66	1.16	0.8	0.09	0.08	1.76	95.61	6	68	26	102	29
1337	50.32	14.65	14.09	4.77	10.23	1.95	0.14	1.18	0.08	0.23	2.94	100.58	7.2	86	34	127	2.4
1403	62.04	14.39	4.51	2.96	5.42	3.92	1.21	2.02	0.37	0.06	1.99	98.89	12	184	84	61	33
1412	51.3	14.97	10.24	4.85	14.73	2.15	0.08	0.68	0.1	0.25	0.13	99.48	4.1	72	13	189	2.3
1413	56.44	17.13	4.04	4.83	9.45	5.41	0.24	0.84	0.05	0.06	0.3	98.79	5.8	89	24	192	6.8
2880	48.1	12.81	13.26	7.63	9.32	0.63	0.08	0.94	0.07	0.2	5.32	98.36	6.5	85	31	76	4.3
2881	48.39	16.2	11.09	6.59	7.6	2.95	0.13	0.87	0.08	0.16	5.35	99.41	4.9	66	14	104	4.9
basalt																	
1255b	47.7	14.9	11.8	4.17	8.71	3.76	0.31	0.7	0.04	0.19	6.6	98.88	14	23	10	51	8.5
1255c	56.4	11.9	16.1	2.89	4.17	2.66	0.21	1.66	0.25	0.09	3.1	99.43	26	206	48	119	14
1255d	56.81	13.67	13.52	4.4	1.88	3.58	0.7	2.31	0.18	0.06	3.13	100.24	7.4	105.5	48	62.3	26.1
1256	49.44	11.1	14.14	2.91	11.62	0.88	0.98	1.63	0.19	0.12	7.48	100.49	8	117	47	63	30
1257	48.79	16.66	18.09	3.88	5.19	0.79	2.17	0.84	0.23	0.11	3.73	100.48	7.6	78	17	75	64
1258	42.88	21.26	18.99	5.42	3.17	4.13	0.38	1.06	0.02	0.14	3.6	101.05	3.5	44.1	9.2	99	11.2
1259	46.25	14.44	12.57	4.9	9.3	3.29	0.2	0.71	0.04	0.19	8.05	99.94	3.4	28	15	70	7.5
1317	43.2	15	12.5	9.54	8.61	1.58	0.05	0.71	0.04	0.18	7	98.41	14	11	10	50	10
1385b	53.3	13.4	10.8	4.78	6.98	3.16	0.19	1.09	0.09	0.2	6.42	100.41	22	107	37	66	10
1377	50.7	14.4	12.5	6.68	8.75	2.02	0.3	1.14	0.09	0.19	2.15	98.92	13	115	34	92	13
1365	50.4	13.8	12.9	6.96	7.44	2.76	0.12	1.11	0.08	0.22	2.75	98.54	35	74	24	63	12
1363	50.6	13.2	13.1	6.49	8.76	2.74	0.17	1.08	0.08	0.22	2.7	99.14	15	69	20	58	11
1361	48.8	11.4	17.9	5.14	5.6	2.01	0.33	0.96	0.09	0.18	3.2	95.61	11	114	34	34	9
1360	44.1	14	10.6	5.86	9.69	1.45	2.43	0.93	0.09	0.17	9.85	99.17	23	89	21	190	47
1319	41.9	13.2	20	6.96	7.88	0.3	0.63	0.68	0.04	0.24	4.65	96.48	15	34	11	35	36
2890	52.9	12.7	17.8	5.83	2.62	1.26	0.23	1.1	0.1	0.17	4.45	99.16	23	122	31	10	10

Compositions are expressed in wt.% (majoe element oxides) and ppm (Nb, Zr, Y, Sr and Rb).

cannot explain the progressive increase of modal quartz contents in the proximal zones by the addition of SiO_2. The quartz enrichment may be more due to an intense destruction of ferromagnesian minerals, as it is observed and noted in many VMS and gold-mineralization environments (O'Hara 1988).

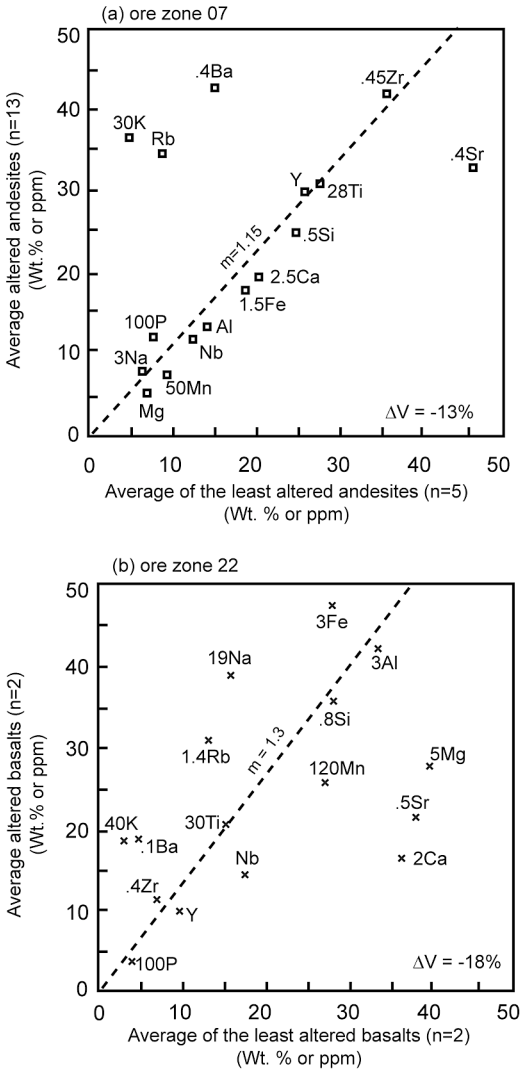

FIG. 9. (a) and (b) Isocon diagrams (Grant 1986) in which the least-altered metabasic rocks are compared to altered ones in the proximal zones. Concentrations are scaled arbitrarily to fit in the diagram (*e.g.,* Ca × 2.5; Ba/10). Elements are expressed as oxides and represented on the diagram as a symbol; Fe_t represents total iron. The slope of each isocon is indicated as a value m used to calculate mass or volume loss (with density).

Chlorite and biotite compositions

Chlorite from several locations at Mouska displays only minor variations in composition. The Fe/(Fe + Mg) ratio and the Si and Al contents of chlorites display a limited range of values corresponding to the "ripidolite" field of Hey (1954). Biotite has been analyzed in basaltic and andesitic samples from proximal zones of alteration. In unaltered metabasic rocks and distal zones of alteration, it is rare, fine-grained, and severely retrograded to chlorite, and generally gives invalid compositions and stoichiometries. However, eighty-eight syntectonic to post-tectonic samples of biotite were analyzed. Unlike chlorite, analyses of biotite in altered samples show clear compositional variations between basaltic and andesitic lithologies (Fig. 10), although they all plot in the biotite field of Deer *et al.* (1962). The Fe/(Fe + Mg) ratio is higher in the andesites than in the basalts, implying that biotite composition depends upon the prevailing local lithology (basalt *versus* andesite), and reflects a chemical contrast in proximal alteration of basalt and andesite (Fig. 10). The proximal alteration of basalt is distinguished by the progressive increases of quartz and white mica (K addition), coincident with a decrease in biotite (K–Mg losses). The overall content of iron in altered andesite is higher than in basalt, accounting for the higher Fe/(Fe + Mg) value of biotite in the andesite.

SULFUR AND OXYGEN ISOTOPE SIGNATURES

To evaluate the source of sulfur in the deposit, a total of 20 mineral separates from 12 samples were analyzed for their sulfur isotopes. The analyses included pyrrhotite, chalcopyrite and pyrite I from the 07, 08 and 22 ore zones and their adjacent proximal zones of alteration. Table 4 and Figure 12 show that the $\delta^{34}S$ values

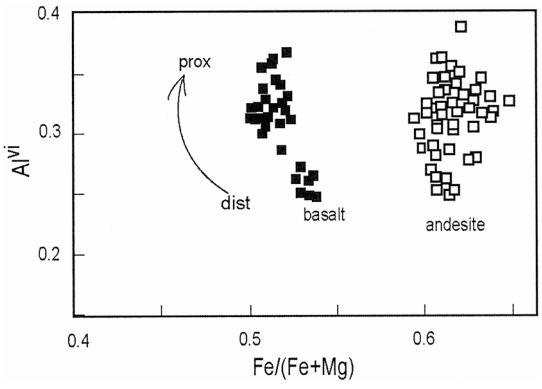

FIG. 10. Fe/(Fe + Mg) *versus* ^{VI}Al in biotite from distal (dist) to proximal (prox) zones of alteration.

cluster around 1.8 to 2‰. The narrow range of $\delta^{34}S$ values is similar to those reported from other gold deposits in the Bousquet area and elsewhere in the Abitibi greenstone belt (Kerrich 1987, Colvine *et al.* 1988, Hoy *et al.* 1988, Hoy & Trudel 1989, Trudel *et al.* 1989, Marquis *et al.* 1990a, b, Gaboury *et al.* 2000). This narrow range and the similarity to magmatic values ($\delta^{34}S \approx 0$‰; Ohmoto & Rye 1979) are consistent with a source of S that was dominantly magmatic, remaining unchanged throughout the hydrothermal process. The sulfur was probably derived by leaching of igneous rocks (Kerrich 1987).

Oxygen isotope analyses were conducted on whole-rock samples and mineral separates of quartz, chlorite, epidote, magnetite and biotite (20 bulk-rock samples and 19 mineral separates) to determine the possible origins and thermal conditions of hydrothermal fluids associated with their deposition. Five samples were collected from the Mic Mac gold mine adjacent to Mouska (see Belkabir *et al.* 1998, Fig. 1), to characterize the trend of oxygen isotope values across the Mouska metabasic rocks of that property.

Bulk-rock analyses were performed on splits taken from the powdered samples used for elemental analysis, whereas the mineral separate samples were obtained by heavy-liquid, Franz electromagnetic, and manual-separation techniques performed on coarsely ground (50–150 mesh) rock splits. Visual examination and X-ray-diffraction analyses confirmed that the mineral separates are at least 95% monomineralic. Extractions of oxygen were performed using the BrF_5 technique of Clayton & Mayeda (1963). All samples were analyzed using a Nuclide 6–60 RMS triple-collector mass spectrometer. All results are reported as δ values relative to the SMOW standard. The analytical precision is approximately ±0.2‰ at a 90% confidence limit.

TABLE 4. SULFUR ISOTOPE DATA DESCRIBING SAMPLES FROM SULFIDE VEINS AND QUARTZ VEINS IN THE MOUSKA DEPOSIT, BOUSQUET DISTRICT, ABITIBI GREENSTONE BELT, QUEBEC

	$\delta^{34}S$ Po	$\delta^{34}S$ Cp	$\delta^{34}S$ Py	T (°C)
1452 sv	2.0			
1288 sv		1.6		
480 qv			2.5	
2883 sv	2.2			
1466 sv	2.0			
1466 sv	1.8			
1291 qv	1.6			
1291 qv		1.7		
1291 qv		1.6		
1258 qv			2.2	
1258 qv	1.8			596.45 ± 63
1341 sv		8.2		
1341 sv	1.6			
1341 sv		1.6		
1467 sv	2.2			
1354 sv	1.1			
1354 sv			1.8	536.40 ± 25
479 qv			4.5	

Sulfur isotope ratios are reported as $\delta^{34}S$, in ‰ relative to the Canyon Diablo troilite (CDT) standard, determined on SO_2 gas extracted by high-temperature combustion of the sulfide with cupric oxide; analyses were carried out at OCGC Stable Isotope Laboratory, Geoscience Centre, Ottawa; precision of analysis was evaluated by duplicate analyses; difference in duplicate $\delta^{34}S$ values is less than ±0.2‰; equilibrium temperatures were calculated from formulas of Ohmoto & Rye (1979).

Bulk-rock samples range in value from 6.3 to 10.7‰ (Table 5); the average of $\delta^{18}O$ values for least-altered metabasic rocks (6.5‰) falls within the normal range for rocks of these compositions (*e.g.,* 5.5 to 7.5‰: Taylor 1968) and is lower than the average $\delta^{18}O$ values for altered and deformed metabasic rocks (7.9‰) (Table 5). These isotopic changes suggest that alteration and deformation occurred under open conditions (*i.e.,* the metabasic rocks were able to exchange oxygen and other components with an external reservoir), presumably as a consequence of fluid migration through the ore zones during deformation. The isotopic compositions of quartz are quite similar those reported elsewhere in the metabasic rocks of the Bousquet area (Hoy & Trudel 1989; Fig. 2).

Quartz–epidote, quartz–calcite, quartz–magnetite, quartz–chlorite and quartz–biotite mineral pairs were analyzed from veins and wallrocks, from distal to proximal zones of alteration, in order to estimate the temperature of hydrothermal activity based on oxygen isotope fractionation (Table 5). The presumed equilibrium oxygen isotope temperature for all pairs ranges from 240 to 420°C, with an average of 320°C. These temperatures are similar to those in other deformed and metamorphosed gold deposits of the Bousquet district (Mic Mac, Mooshla A, Doyon and Dumagami; see Hoy & Trudel 1989). Oxygen isotope data, supplemented in part by fluid-inclusion studies (Trudel *et al.* 1989), suggest that deformation at all of these deposits involved the passage of fluids having $\delta^{18}O$ values of 2 to 6‰ at a temperature between about 250 and 400°C (Eliopoulos 1983, Trudel *et al.* 1989, Hoy 1991). The values bracket those suggested for the deformation and mineralization at Mouska ($300 < T < 400$°C, respectively; $\sim 0.4 < \delta^{18}O < 6$‰). Temperature and $\delta^{18}O$ values for fluids in this range would have produced bulk-rock values of 6 to 9‰ $\delta^{18}O$ for the altered rocks.

Discussion

The emplacement of gold

Genetic interpretations of the gold–sulfide associations in volcanic-rock-associated massive and disseminated sulfide deposits of the Bousquet mining district have been a long-standing problem and the source of much controversy for more than a decade. Gold has been interpreted to be syngenetic (*e.g.,* Valliant *et al.* 1983, Bateman 1984), to consist of epithermal remobilization during a multistage syn- to late-tectonic event (Tourigny *et al.* 1989a, b, 1993), or to be epigenetic and related spatially to synvolcanic exhalative Fe–Cu–Zn deposits (Guha *et al.* 1982, Marquis *et al.* 1990a, b). Because of the intense tectonometamorphic overprint recorded in most of the deposits in the Bousquet area, the internal distribution of premetamorphic mineralization must

have been extensively reworked, and original relationships between gold and sulfides would have been largely obliterated if the gold emplacement predated metamorphism and deformation. In the Mouska deposit, this tectonometamorphic imprint has been relatively less intense (Belkabir & Hubert 1995), and some exceptional primary relationships between gold and sulfides have been preserved. In fact, the mineralogical investigation of the deposit clearly reveals a genetic link between gold and premetamorphic sulfides. This interpretation is based on the textural relationships between microinclusions of gold and their host pyrite (fine-grained, type-I pyrite). In this case, the gold at Mouska is considered to be syngenetic in origin and to have been partly remobilized into brittle structural sites (veins) during dynamic metamorphism (*cf.* Hilmy & Osman 1989). Variations in Au:Ag values between primary gold and gold encountered elsewhere in the ore zones corroborate this interpretation. With its progressive reworking during metamorphism and deformation, gold displays

TABLE 5. OXYGEN ISOTOPE COMPOSITIONS OF SAMPLES OF MINERAL SEPARATES FROM VEINS AND ADJACENT WALLROCK, MOUSKA DEPOSIT,BOUSQUET DISTRICT, ABITIBI GREENSTONE BELT, QUEBEC

	Description	$\delta^{18}O_{SMOW}$ ‰						T°C; Fluid $\delta^{18}O$				
		WR	Qtz	Mgt	Chl	Bt	Ep	Qtz -Ep	Qtz -Cal	Qtz -Mgt	Qtz -Chl	Qtz -Bt
1258	Po, Bt, Chl vein (zone 07)		10.5		2.3		6.3	360-5.6		240-1.1		
475	Felsic tuff		9.1		3.9	5.3; 5.49ms			410-5.3	270-1 290-2		
480a	Qtz, Py, Mgt, veinlets (zone 22)		10.6	0.3	4.11	3.22		320-4.4			420-7	300-4
480b	Magnetic basalt (zone 22)		9.2		0.9				240-0.4			
479a	altered basalt (zone 22)		10.5				5.2	300-3.7				
479b	Late Qtz-Py vein		8.9									
1288	Massive Cp vein with Qtz (zone 08)		10.3									370-5.6
2883	Po vein with Qtz, Bt, Chl (zone 08)		8.3 10.6,10.4			3.4						
1291a	Qtz-Po-Cp vein (zone 08)		9.4,9.4			4.21					370-5.6	
1291b	Qtz-Po-Cp vein with chlorite (zone 08)		7.5,9.9			4.24						
1341	Po-Cp vein with Bt-Qtz-Chl (zone 07)		10.4		3.8§	3.2					310-4	360-5.3
1467	Po vein with Bt-Qtz-Cal (zone 07)		8.12,7									
470	Chloritized diorite dike		10.5		3.4						290-3.2	
92-01	Milky qtz (Mic Mac mine)*		10									
92-02	Au-Qtz vein (Mic Mac mine)		10.5									
92-03	Wallrock with biotite alteration (Mic Mac mine)					2.7						320-4.7 350-4.8
92-04	Qtz-Po-Cp vein (Mic Mac mine)		11.0,10.6									
92-05	Qtz vein with Cp-Mgt (Mic Mac)		8.9,8.6									
302	Weakly altered basalt	6.4										
304	Qtz-Ab tuff	7.6										
421	Silicified basalt	6.4										
470	Chl diorite dike	6.3										
1403	Chl andesite	9.0,10.7										
1321	Mgt-Bt schist	8										
1407	Silicified magnetic basalt	8.7										
1408	Qtz-Py veined basalt	6.3										
1409	Bt basalt	7.4										
1383	Weakly altered andesite	6.6										
1384a	Cp-Po-Qtz-Bt vein	8.4										
1384b	Bt andesite	6.4										
1385a	Weakly altered andesite	6.6										
2891	Po-Cp veinlets in massive andesite	9.9,9										
2876	Weakly altered andesite	6.7										
1255d	Bt-Mgt basalt	7.1										
1256	Phyllonitic ore basalt (zone 22)	8										
1257	Phyllonitic ore basalt (zone 22)	6,7										
1258	Phyllonitic ore basalt (zone 22)	10										
1259	Phyllonitic ore basalt (zone 22)	7.7										

* Belkabir & Hubert (1995, Fig. 1). § Replicated. WR: whole rock.

an enrichment in Ag. Values of Au:Ag, used in several sulfide-rich gold deposits throughout the world as an effective means to classify gold mineralization (Fleming *et al.* 1986, Shikazono & Shimizu 1987, Proudlove & Hutchinson 1987) may vary with variations in physicochemical conditions [T, P, pH, Eh, $f(O_2)$, $f(S_2)$, *etc.*] and may thus reflect a possible multistage emplacement of gold. In the nearby Noranda mining camp, Larocque & Hodgson (1993) demonstrated that primary gold is refractory and associated with the primary facies of mineralization in the weakly deformed Mobrun volcanic-rock-associated massive-sulfide deposit. The gold was further remobilized during subsequent metamorphism and deformation so that it became more recoverable. On the other hand, gold in many highly deformed deposits, such as those in the Bousquet district (*e.g.,* the Bousquet I, Bousquet II and Dumagami deposits), is consistently found in later syntectonic sites (*e.g.,* veins and veinlets) and therefore represents remobilized gold. These concepts undoubtedly apply as well to the strongly deformed portions of the Mouska mineralization.

Timing of alteration and mineralization

The mineral assemblages surrounding the Mouska ore zones (alteration halos) result from the complex and progressive interaction between hydrothermal and predeformational phenomena (sulfide event) and tectonometamorphic (quartz event) imprints. The observed contrast in alteration and mineralization between andesite and basalt lithologies is enhanced by the first hydrothermal-predeformational event. Belkabir & Hubert (1995) showed that sulfide mineralization in the Mouska deposit was reworked during dynamic metamorphism and that it was clearly premetamorphic in origin. Sulfide mineralization in the andesites was emplaced largely as veins (massive to semimassive) within a biotite-rich proximal zone of alteration. Mass-balance calculations in the andesites and basalts show an increase in K with increasing intensity of alteration, accompanied by almost undisturbed silica contents. In basalt, the proximal alteration is more complex, characterized by progressively increasing modal quartz and formation of white mica toward the ore-bearing schist, replacing both biotite and chlorite. Pyrite in association with magnetite in basalt suggests a lower $a(H_2S)$ in the hydrothermal fluid (*cf.* Barton & Skinner 1979). On the other hand, "silicification", seen as microcrystalline quartz accompanying magnetite, suggests a higher $a(O_2)$ in the associated fluid (Barnes 1979). This environment is clearly favorable for the deposition of pyrite-rich assemblages, compared to proximal alteration of andesitic lithologies where pyrite is less prominent, and the sulfides consist essentially of pyrrhotite and chalcopyrite. Silicification, found in association with mineralization in basaltic lithologies, can also explain the disseminated nature of the 22 ore zone. Assuming that silicification is in part premetamorphic, it could have sealed early fractures of basalt, resulting in a limited flow of fluid and, consequently, a less important host for sulfide deposition during the pre-metamorphic alteration (*cf.* Theart *et al.* 1989).

Acknowledgements

This paper is based on a Ph.D. thesis, conducted by the first author at the Université de Montréal. Funding was provided by Cambior Inc. and a Natural Sciences and Engineering Research Council of Canada. This study would not have been possible without the generous assistance of the staff of the Mouska mine. We are very grateful also to F. Robert of Barrick Gold Co. for many fruitful discussions and to W.H. MacLean and Alex Brown for their review of an earlier version of this paper. Constructive and very thorough reviews by Drs. Gema Olivo and David Lentz are gratefully acknowledged.

References

Barnes, H.L. (1979): Solubilities of ore minerals. *In* Geochemistry of Hydrothermal Ore Deposits (H.L. Barnes, editor, 2nd ed.). Wiley Interscience, New York, N.Y. (404-459).

Barton, P.B., Jr. & Skinner, B.J. (1979): Sulfide mineral stabilities. *In* Geochemistry of Hydrothermal Ore Deposits (H.L. Barnes, editor, 2nd ed.). Wiley Interscience, New York, N.Y. (278-403).

Belkabir, A. & Hubert, C. (1995): Geology and structure of a sulfide-rich gold deposit: an example from Mouska gold mine, Bousquet district, Canada. *Econ. Geol.* **90**, 1064-1079.

_____, _____ & Hoy, L. (1998): Fluid-rock reactions and resulting change in rheological behavior of a composite granitoid: the Archean Mooshla stock, Canada. *Can. J. Earth Sci.* **35**, 131-146.

Clayton, R.N. & Mayeda, T.K. (1963): The use of bromine pentafluoride in the extraction of oxygen from oxides and silicates for isotopic analysis. *Geochim. Cosmochim. Acta* **27**, 43-52.

Colvine, A.C., Fyon, J.A., Heather, K.B., Marmont, S., Smith, P.M. & Troop, D.G. (1988): Archean lode gold deposits in Ontario. *Ont. Geol. Surv., Misc. Pap.* **139**.

Deer, W.A., Howie, R.A. & Zussman, J. (1962): *Rock-Forming Minerals*. 3. *Sheet Silicates*. Longman, New York, N.Y.

Eliopoulos, D.G. (1983): *Geochemistry and Origin of the Dumagami Pyritic Gold Deposits, Bousquet Township, Quebec.* M.Sc. thesis, Univ. of Western Ontario, London, Ontario.

Fleming, A.W., Handley, G. A., Williams, K.L., Hills, A.L. & Corbett, G.J. (1986): The Porgera gold deposit, Papua, New Guinea. *Econ. Geol.* **81**, 660-680.

FLOYD, P.A. & WINCHESTER, J.A. (1978): Identification and discrimination of altered and metamorphosed volcanic rocks using immobile trace elements. *Chem. Geol.* **21**, 291-306.

FRATER, K.M. (1984): Mineralization at the Golden Grove Cu–Zn deposit, Western Australia. II. Deformation textures of the opaque minerals. *Can. J. Earth Sci.* **22**, 15-26.

GABOURY, D., DAIGNEAULT, D. & BEAUDOIN, G. (2000): Volcanogenic-related origin of sulfide-rich quartz veins: evidence from O and S isotopes at the Géant Dormant gold mine, Abitibi belt, Canada. *Mineral. Deposita* **35**, 21-36.

GALLEY, A.G., PILOTE, P. & DAVIS, D. (2003): Gold-related, subvolcanic, Mooshla intrusive complex, Bousquet mining district, Quebec. *Geol. Assoc. Can. – Mineral. Assoc. Can., Program Abstr.* **28**.

GRANT, J.A. (1986): The isocon diagram – a simple solution to Gresen's equation for metasomatic alteration. *Econ. Geol.* **81**, 1976-1982.

GUHA, J., GAUTHIER, A., VALLÉE, M., DESCARREAUX, J. & LANGE-BRARD, F. (1982): Gold mineralization patterns at the Doyon mine (Silverstack), Bousquet, Quebec. *In* Geology of Canadian Gold Deposits (R.W. Hodder & W. Petruk, eds.). *Can. Inst. Mining Metall., Spec. Vol.* **24**, 50-57.

HEY, M.H. (1954): A new review of the chlorites. *Mineral. Mag.* **30**, 277-292.

HILMY, M.E. & OSMAN, A. (1989): Remobilization of gold from a chalcopyrite–pyrite mineralization Hamash gold mine, Southeastern Desert, Egypt. *Mineral. Deposita* **24**, 244-249.

HOY, L.D. (1991): Regional evolution in oxygen isotopic composition of hydrothermal fluids associated with base metal sulfide deposits, Noranda, Quebec. *Geol. Assoc. Can. – Mineral. Assoc. Can., Program Abstr.* **16**, A57.

_____, KHEANG, L. & TRUDEL, P. (1988): Evidence from fluid inclusion and stable isotope studies for the thermochemical nature of fluids responsible for Au mineralization in Bousquet Township, Quebec. *Geol. Assoc. Can. – Mineral. Assoc. Can., Program Abstr.* **13**, A58.

_____ & TRUDEL, P. (1989): Evidence for regional hydrothermal processes in the development of Au mineralization in and around Bousquet Township, Québec. *Geol. Assoc. Can. – Mineral. Assoc. Can., Program Abstr.* **14**, A91.

KERRICH, R. (1987): The stable isotope geochemistry of Au–Ag vein deposits in metamorphic rocks. *In* Stable Isotope Geochemistry of Low Temperature Fluids (T.K. Kyser, ed.). *Mineral. Assoc. Can., Short Course* **13**, 287-336.

LAROCQUE, A.C.L., HODGSON, C.J. & LAFLEUR, P.-J. (1993): Gold distribution in Mobrun volcanic-associated massive sulfide deposit, Noranda, Quebec: a preliminary evaluation of the role of metamorphic remobilization. *Econ. Geol.* **88**, 1443-1459.

MACLEAN, W.H. & KRANIDIOTIS, P. (1987): Immobile elements as monitors of mass transfer in hydrothermal alteration: Phelps Dodge massive sulfide deposit, Matagami, Quebec. *Econ. Geol.* **82**, 951-962.

MARQUIS, P., BROWN, A.C., HUBERT, C. & RIGG, D.M. (1990b): Progressive alteration associated with auriferous massive sulfide bodies at the Dumagami mine, Abitibi greenstone belt, Quebec. *Econ. Geol.* **85**, 746-764.

_____ & HUBERT, C., BROWN, A.C. & RIGG, D.V. (1990a): Overprinting of early, redistributed Fe and Pb–Zn mineralization by late-stage Au–Ag–Cu deposition at the Dumagami mine, Bousquet district, Abitibi, Quebec. *Can. J. Earth Sci.* **27**, 1651-1671.

_____, _____, _____ & _____ (1990c): An evaluation of genetic models for gold deposits of the Bousquet district, Quebec, based on their mineralogic, geochemical and structural characteristics. *In* The Northwestern Quebec Polymetallic Belt (M. Rive, P. Verpaelst, Y. Gagnon, J.-M. Lulin, G. Riverin & A. Simard, eds.). *Can. Inst. Mining Metall., Spec. Vol.* **43**, 383-399.

NGUYEN, P.T., BOOTH, S.A., BOTH, R.A. & JAMES, P.R. (1988): The White Devil gold deposit, Tennant Creek, Northern Territory, Australia. *Econ. Geol., Monogr.* **6**, 180-192.

O'HARA, K.D. (1988): Fluid flow and volume loss during mylonitisation: an origin for phyllonite in an overthrust setting, North Carolina, U.S.A. *Tectonophys.* **156**, 21-36.

OHMOTO, H. & RYE, R.O. (1979): Isotopes of sulfur and carbon. *In* Geochemistry of Hydrothermal Ore Deposits (H.L. Barnes, ed.). Wiley Interscience, New York, N.Y. (509-567).

PROUDLOVE, D.C. & HUTCHINSON, R.W. (1987): Multiphase mineralization in concordant and discordant gold veins, Dome mine, South Porcupine, Ontario, Canada. *Econ. Geol., Monogr.* **6**, 112-123.

RICKARD, D.T. & ZWEIFEL, H. (1975): Genesis of Precambrian sulfide ores, Skellefte district, Sweden. *Econ. Geol.* **70**, 225-274.

SHIKAZONO, N., & SHIMIZU, M. (1987): The Ag/Au ratio of native gold and electrum and the geochemical environment of gold vein deposits in Japan. *Mineral. Deposita* **22**, 309-314.

STANTON, R.L. (1972): *Ore Petrology*. McGraw-Hill, New York, N.Y.

STONE, W.E. (1988): *Nature and Significance of Metamorphism in Gold Concentration, Bousquet Township, Abitibi Greenstone Belt, Northwest Quebec.* Ph.D. thesis, Univ. of Western Ontario, London, Ontario.

TAYLOR, H.P., JR. (1968): The oxygen isotope geochemistry of igneous rocks. *Contrib. Mineral. Petrol.* **19**, 1-71.

THEART, H.F.J., CORNELL, D.H. & SCHADE, J. (1989): Geochemistry and metamorphism of the Prieska Zn–Cu deposit, South Africa. *Econ. Geol.* **84**, 34-48.

TOURIGNY, G., BROWN, A.C., HUBERT, C. & CRÉPEAU, R. (1989a): Synvolcanic and syntectonic gold mineralization at the Bousquet mine, Abitibi greenstone belt, Quebec. *Econ. Geol*. **84**, 1875-1890.

_____, DOUCET, D. & BOURGET, A. (1993): Geology of the Bousquet 2 mine: an example of a deformed, gold-bearing, polymetallic sulfide deposit. *Econ. Geol.* **88**, 1578-1597.

_____, HUBERT, C., BROWN, A.C. & CRÉPEAU, R. (1988): Structural geology of the Blake River Group at the Bousquet mine, Abitibi, Quebec. *Can. J. Earth Sci.* **25**, 581-592.

_____, _____, _____ & _____ (1989b): Structural control of gold mineralization at the Bousquet mine, Abitibi, Québec. *Can. J. Earth Sci.* **26**, 157-175.

TRUDEL, P., SAUVÉ, P., TOURIGNY, G., HUBERT, C. & HOY, L. (1989): Caractéristiques géologiques des gisements d'or du secteur de Cadillac, Abitibi, Québec. *Ministère de l'Énergie et des Ressources Québec*.

VALLIANT, R.I., BARNETT, R.L. & HODDER, R.W. (1983): Aluminum silicate-bearing rock and its relation to gold mineralization, Bousquet mine, Bousquet Township, Quebec. *Can. Inst. Mining Metall., Bull.* **76**(850), 81-90.

VOKES, F.M. (1969): A review of the metamorphism of sulfide deposits. *Earth Sci. Rev.* **5**, 99-143.

WILHELMEY, J.F. (1987): Minéralogie de l'or de la propriété Mouska. Internal Report, Cambior Inc., **87–Mi–020**.

Received November 15, 2003, revised manuscript accepted July 21, 2004.